



# A Novel an All-Optical Refractive Index Biosensor Based-on Glass Cylinder Cavity Resonance for Detection of Malaria-Infected Red Blood Cells

Gregory T. MacLennan<sup>1,\*</sup>

<sup>1</sup>School of Medicine, Case Western Reserve University, Cleveland OH 44106, USA

## Highlights

- Design of an all-optical biosensor for early detection of malaria disease.
- Optical biosensors based on 2D photonic crystals offer faster and more accurate detection.
- Biosensor measures the refractive index of healthy and infected samples in the human body.
- Sensitivity parameter calculated as a percentage (%RIU-1) for different detection modes.
- Proposed biosensor utilizes finite difference time domain method and has compact dimensions (57 $\mu\text{m}^2$ ) for improved speed and reduced time delay.

## Article Info

Received: 26 April 2023  
 Received in revised: 06 June 2023  
 Accepted: 06 June 2023  
 Available online: 29 June 2023

## Keywords

Optical Biosensor,  
 High-Sensitivity,  
 Photonic Crystal,  
 Refractive Index,  
 Sensitivity,  
 Malaria,  
 Red Blood Cells,  
 2D-FDTD.

## Abstract

Malaria mosquitoes are abundant in most countries with warm climates, so malaria disease spreads rapidly through the bites of these mosquitoes to the human body. The effects of these diseases are very dangerous and deadly. Early detection of such diseases is very important to prevent death. In this paper, an all-optical biosensor based on the refractive index of healthy and infected samples in the human body is designed and presented. Many biosensors have been introduced in various ways in recent years, but optical biosensors based on two-dimensional photonic crystals (2D-PhCs) have received less attention for the detection of malaria disease. The proposed biosensor has a faster and more accurate detection than previous works. In addition, the sensitivity parameter is calculated as a percentage. The main function of the biosensor is based on the intensity of the signal transmitted from the input waveguide to the output waveguide. The higher the intensity of the received signal, the better for the person. The range of percentages is between 97% ~ 66.12% and the range of sensitivity is between 8.21RIU-1 ~ 11.91 RIU-1. In previous similar articles, sensitivity has not been calculated as a percentage, but here, due to showing the amount of sensitivity in different modes, the sensitivity parameter is defined as %RIU-1. The interaction of light with matter and samples of Maxwell's functional equations, and to obtain the output results in the software, the finite difference time domain method in two-dimensional is used. The overall dimensions of the proposed biosensor are very small and 57 $\mu\text{m}^2$ , which reduces the time delay and increases the speed

## 1. Introduction

### 1.1. Photonic Crystals (PhCs)

Photonic crystals (PhCs) are dielectric rods that are arranged in the same order and shape in this paper. Due to their unique properties, including flexibility, and wide wavelength range, control of optical signals in regions. Custom is known as a suitable environment for designing

all-optical devices [1]. In addition, the photonic has very important properties such as bandgap (PBG), speed of light, and no noise, which can be a significant advantage over the electronic, and expand PhCs-based applications. Recently, researchers have been trying to design almost all electronic devices as PhCs-based all-optical devices, which so far have a wide variety of PhCs-based structures such as

\* Corresponding Author: Augustinus Sieck  
 Email: [gregory-maclennan@case.edu](mailto:gregory-maclennan@case.edu)

Optical biosensors [2-4], Optical filters [5,6], Optical demultiplexers [8,9], Optical flip-flops [10-12], Optical flip-flops [13,14], and Optical analog-to-digital converters [15,16], have been proposed.

### **1.2. Optical Biosensors**

Optical Biosensors are considered analytical detectors that detect different types of diseases by using the refractive index of samples and the interaction of light and matter [17]. Bio-photonic sensors have many advantages that distinguish them from conventional diagnostic techniques, such as single-stage detection, ease of use, and most biosensors that allow better and faster control over measurement. There are different types of biosensors such as electrical, piezoelectric, electrochemical, nanomechanical, magnetic, acoustic, and optical [18-21]. The optical transducer mechanism is a system that modulates the interaction with optical radiation in a recognizable manner. Because a special photonic structure that can be used for measurement is a photon crystal (PC), in this paper, we present a highly sensitive 2D-PhC-based biosensor structure with an input waveguide, an output waveguide, and a glass cylinder, which the samples are placed is designed [22].

### **1.3. Malaria**

Malaria is the leading cause of morbidity and mortality worldwide, affecting more than 500 million cases of fever and approximately 1 million deaths per year. The disease is usually transmitted by Anopheles mosquitoes and infected material. The disease enters the body through mosquito bites, parasites that are present in the mosquito saliva. The parasites go to the liver and grow and reproduce there. There are five types of infected Plasmodium that can be transmitted by humans. Plasmodium types are P falciparum, P vivax, P ovale, P malaria and P Knowlesi. The most dangerous type is P falciparum. Plasmodium and infected Anopheles mosquito and the dangerous substance sporozoite into human blood, which is very deadly.

As mentioned earlier, mosquitoes often suck and feed on human blood. By biting, sporozoites are a type of malaria parasite that is injected into human tissues through the blood. They usually damage liver cells. Merozoites, on the other hand, enter the bloodstream to damage red blood cells. [23]. When merozoites flow into the bloodstream, they cause biochemical changes in red blood cells and eventually turn into mononuclear trophozoites. In the schizoprenic stage, trophozoites become multinucleated cells called schizonts. Schizont growth is based on the digestion of hemoglobin by the production of hemozoin. [24]. Most blood tests are more sensitive tests for malaria infection. Using a larger volume of blood under a microscope, more parasites are examined. The result of

such smear tests depends on the quality of the equipment, the result of which is not suitable for large-scale epidemiological studies.

The aim and main issue addressed in the study is the urgent need for an efficient and accurate detection method for malaria disease, which spreads rapidly through mosquito bites and can be deadly. The significance of the research lies in addressing the urgent need for an efficient and accurate detection method for malaria, a disease that poses a significant global health burden. By developing an all-optical biosensor based on 2D-PhCs, the study offers the potential for a faster and more accurate detection approach compared to existing methods. This research has the potential to contribute to early detection of malaria, enabling timely intervention and treatment, thereby reducing morbidity and mortality associated with the disease. To tackle this problem, the paper proposes an all-optical biosensor based on two-dimensional photonic crystals (2D-PhCs).

In this paper, an optical biosensor based on 2D-PhC for malaria diagnosis is presented in five main sections. The first section describes photonic crystals, biosensors, and information on specimens of malaria mosquitoes. The second part deals with the numerical method and calculation of results. The third part of the proposed biosensor is examined. The fourth section discusses the extent of allergies and other outcomes in different malaria samples, and in the last section, the is the conclusion. The proposed biosensor offers faster and more accurate detection by analyzing the refractive index of healthy and infected samples in the human body and measuring the intensity of the transmitted signal.

## **2. Theory and Method**

Photonic crystals (PCs) are composed of dielectric materials with repeated and regular arrangements at equal distances from each other in a bed [6]. In designing and simulating photonic crystals, three types of structures are used: one-dimensional (1D), two-dimensional (2D), and three-dimensional (3D). In this paper, a two-dimensional structure is used in the design. Two-dimensional structures also have two main parts. The first part is the placement of the dielectric rods in the air bed. The second part consists of air cavities created in the dielectric substrate. In designing the proposed structure, the first part and the two-dimensional structure of photon crystals have been used. The phenomenon of light scattering in the software by solving the Maxwell equations given in Eq (1). Calculations of the results and outputs taken related to the structure, using the finite-difference two-dimensional method.

$$\nabla \times \left( \frac{1}{\varepsilon} \nabla \times H \right) = \left( \frac{\omega}{c} \right)^2 H \quad (1)$$

The sensitivity parameter is an important factor in a biosensor. Usually, to calculate the sensitivity of the detection between healthy and unhealthy samples, the difference in resonance wavelengths must be divided by the difference in refractive index. But here, due to the variability of the transmitted power optical signal, instead of the resonant wavelength, we will calculate the sensitivity value from Eq (2).

$$S = \frac{\Delta TE}{\Delta RI} \left( \frac{\%}{RIU} \right) = (0.01 RIU^{-1}) \quad (2)$$

Where  $TE$  is the power transfer rate from the input waveguide to the output waveguide, the unit of which is normalized in percentage (%). The  $RI$  parameter is the refractive index value of the samples, which is indicated by the unit  $0.01 RIU^{-1}$ . As can see, in this work, we calculate the sensitivity value in percentage.

Photonic crystals have many applications in optical communication and optical information processing

because photonic crystals provide a common platform for the construction of a large number of optical components on a chip down [8]. Light is not allowed to pass in the PBG frequency range, it can only be localized by creating certain defects in the structure of the PC, otherwise, the light in the PBG is completely forbidden. These PC bandgap structures can be used for various applications [9].

### 3. Proposed Device

Fig. 1 shows the transmission spectrum in an integrated two-dimensional structure. As mentioned earlier, the pink line shows the frequency of transmission through the integrated structure. This frequency range is between  $a/\lambda = 0.2826 \sim 0.4169$ . The blue line also shows the wavelengths transmitted through the integrated structure. According to the figure of a green area, it is specified that the wavelengths are not allowed to pass and this is the bandgap of the structure. The working range of the integrated structure (green line) is between  $\lambda = 1.199\mu\text{m} \sim 1.769\mu\text{m}$ . The free spectral range of around  $FSR = 570 \text{ nm}$ .

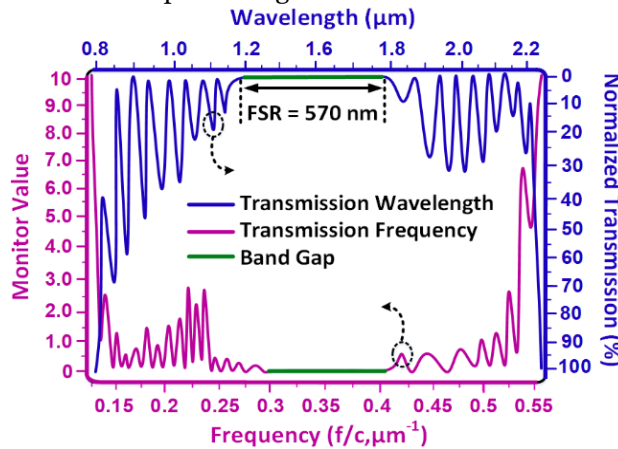


Fig. 1. Frequency transmission spectrum.

In the proposed structure, dielectric rods are made of silicon with the silicon substrate and a refractive index of  $n_{\text{si}} = 3.46$  in the air bed with a refractive index of  $n_{\text{a}} = 1$ . Fig. 2 shows the proposed biosensor in two dimensions or top-view. The lattice index (distance from the center to the center of two adjacent rods) is equal to  $a = 500 \text{ nm}$ . The radius of the dielectric rods is equal to  $r = 0.2a = 100 \text{ nm}$ . The detection operation is performed by the refractive index of the samples that are placed in the green cylinder. The green cylinder is made of ordinary glass with a refractive index and reduce are  $n_{\text{G}} = 1.52$ ,  $R_{\text{C}} = 600 \text{ nm}$  respectively. The red parts represent the samples, which change the amount of light signal received from the output

of the structure by changing them and their refractive index. The pink rods around the cavity are the main ones to increase the accuracy of the detection operation. The yellow light seen in the structure represents the light of the input source and the blue light indicates the change in the amount of light signal transmission. The overall dimensions of the structure are equal to  $57\mu\text{m}^2$ . Due to the small overall dimensions, the proposed structure is capable of assembly and this is an important advantage in the design that the small path of the waves also reduces the length of the optical signal path and thus increases the overall speed in the device.

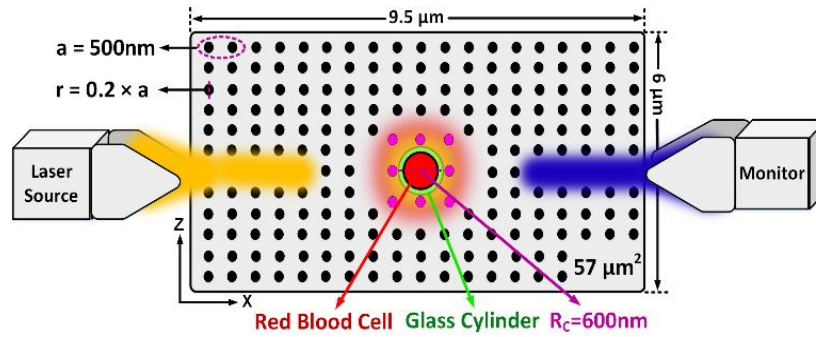


Fig. 2. Top-view of proposed biosensor.

Since in this paper an important parameter for measuring sensitivities is the transmission for different samples, so we will put all the samples in the structure once and calculate the throughput, and then the sensitivity of each unhealthy sample to calculate a healthy sample.

The proposed biosensor for malaria detection employs a compact and efficient two-dimensional photonic crystal structure. The structure comprises silicon rods with a refractive index of 3.46, surrounded by a green glass cylinder with a refractive index of 1.52. By manipulating the refractive index of the samples within the green cylinder, the amount of light signal transmitted through the structure can be controlled. This enables precise detection of malaria-related changes. The compact dimensions of the biosensor, measuring  $57\mu\text{m}^2$ , offer advantages in terms of easy assembly and reduced optical signal path length, resulting in improved speed and performance of the device.

#### 4. Result and Discussion

In this section, important transmission (TE) calculations for each of the normal and Infected samples (Infected red blood cell ring stage, Infected red blood cell trophozoites stage, Infected red blood cell schizont stage) are discussed. As can be seen from Fig. 3, the highest throughput is related to the normal sample with TE = 97%, and the lowest throughput is related to the infected schizont stage sample at TE = 66.12%. Therefore, we can identify the type of samples by the intensity of the light signal that we receive as a percentage of the structure output. The large difference between the values of the transmission makes it easier and more accurate to separate them from each other. One of the important advantages of our proposed structure compared to other similar structures is the high throughput rate of up to 97%, in other words, at best, only 3% of power losses signal in the structure.

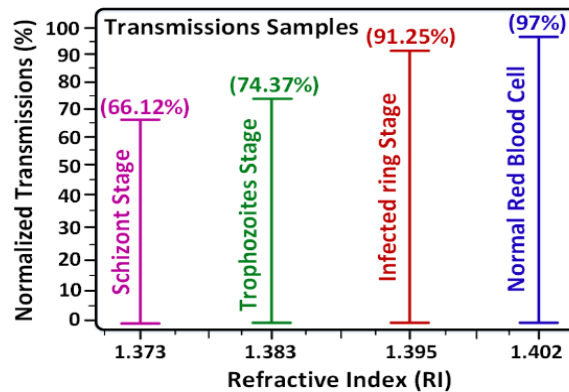


Fig. 3. Transmission spectrum of different red blood cell samples.

Here we want to calculate the sensitivity of a normal sample to infected samples. As mentioned earlier in this paper, due to the change in the intensity of the signal received from the output or the percentage of transmission in the different samples, we also calculate the sensitivity in terms of percentage. Fig. 4 shows the sensitivity of the different refractive index of the samples. As mentioned before, to calculate the sensitivity parameter, we divide the transmission difference by the refractive index difference of

different samples and finally show the sensitivity in percentage. The sensitivity for detecting the infected red blood cell ring stage sample from normal was equal to sensitivity  $S = 821.42 \text{ \%RIU}^{-1} = 8.21 \text{ RIU}^{-1}$ . The sensitivity for infected red blood cell trophozoites stage and infected red blood cell schizont stage samples are  $S = 191.05\% \text{RIU}^{-1} = 11.91 \text{ RIU}^{-1}$  and  $S = 1064.82 \text{ \%RIU}^{-1} = 10.64 \text{ RIU}^{-1}$ , respectively. Then we collected all the calculated results in the form of a table. Table 1 shows the significant values of

sensitivity and transmission for the samples and the different refractive index.

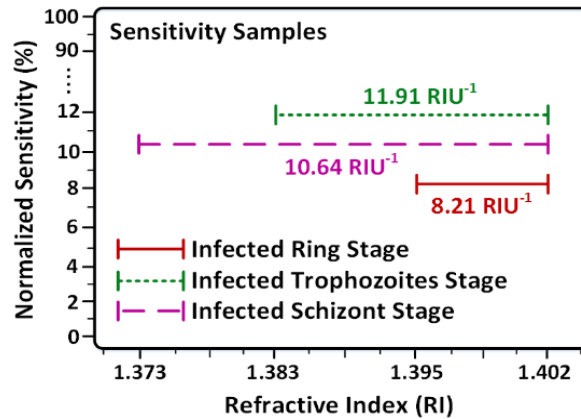


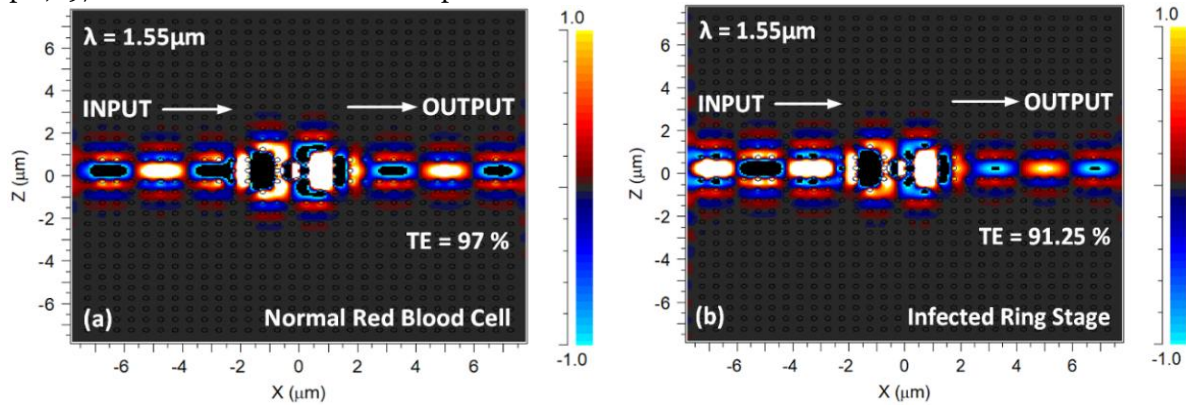
Fig. 4. The Sensitivity Samples.

Table 1. The Sensitivity and transmissions of different refractive index.

Samples	(RI)	TE (%)	S (RIU <sup>-1</sup> )
Normal Red Blood Cell	1.402	97	Ref
Infected Ring Stage	1.395	91.25	8.21
Infected Trophozoites Stage	1.383	74.37	11.91
Infected Schizont Stage	1.373	66.12	10.64

Another important advantage is the structure of the work at wavelength  $\lambda=1.55\mu\text{m}$ , which is the normal central wavelength in most light sources, and it can be concluded that we will have no problem setting the light source with the proposed field. in this section (Fig. 5), to better understand the signal density and transmissions in different samples, the graphic mode is examined. As shown in Fig. 5(a), a continuous Gaussian light signal with a wavelength of  $\lambda=1.55\mu\text{m}$  is applied to the input waveguide of the structure, and after passing through a normal red blood sample, 97% is transferred to the output of the

structure, in which case a 3% of Signal power is lost. In Fig. 5(b), by placing the Infected Ring Stage, the intensity of the output signal is reduced to 91.73%, and 8.27% of the optical signal is lost. In Fig. 5(c), when the infected trophozoites stage sample is placed, the amount of signal intensity at the output reaches 74.37% and we have a power loss of about 25.63%. Finally, in Fig. 5(d), by placing the Infected Schizont Stage sample in the structure, 66.12% of the output of the structure is received, and we have a power loss of about 33.88%.





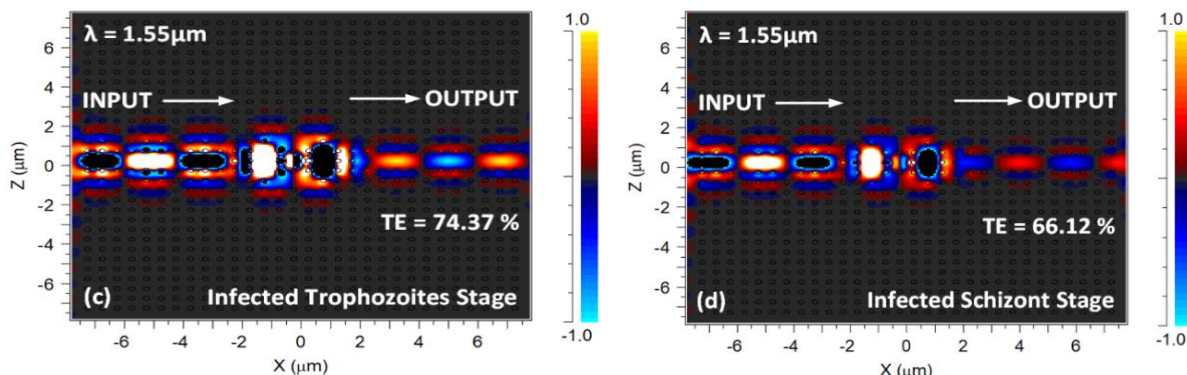


**Fig. 5.** Schematic of structure behavior at different refractive index, (a) Normal red blood cell, (b) Infected ring stage, (c) Infected trophozoites stage, (d) Infected schizont stage.

In this part, in order to prove that the radius of the glass cylinder in which the samples are placed is at its best,  $R_c = 600\text{nm}$ , we performed the calculations for the normal sample at different radii of the glass cylinder. As can be seen in Fig. 6, with increasing the radius of the cylinder to  $R_c < 600\text{ nm}$ , the percentage of transmission power increases,

and after passing the value of  $R_c > 600\text{ nm}$ , the number of transmission power decreases. Therefore, it can be concluded that a radius of  $R_c = 600\text{ nm}$  is the best radius for the cylinder. On the other hand, the lowest power loss is related to the radius of  $600\text{ nm}$ .

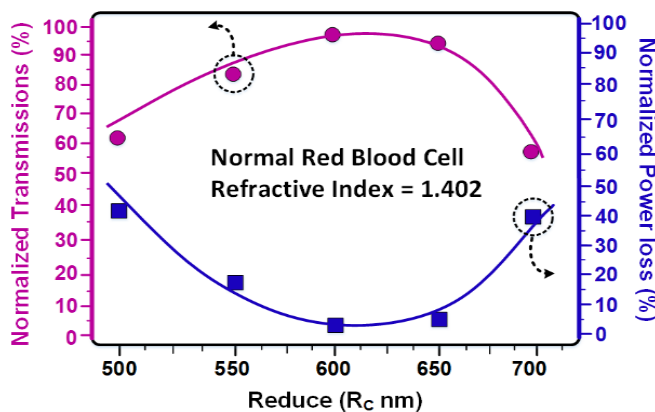


**Fig. 6.** Transmission and power loss in terms of different radius of the glass cylinder.

To be surer in choosing the right radius, in Fig. 7 the sensitivity values for the Infected Ring Stage sample are measured in different cylinder radius. As can be seen, with increasing the radius up to  $R_c < 600\text{ nm}$ , the sensitivity is

almost the same and has increased slightly in the radius of  $R_c = 600\text{nm}$ , and after the radius of  $R_c > 600\text{ nm}$ , the percentage of sensitivity decreases slightly.

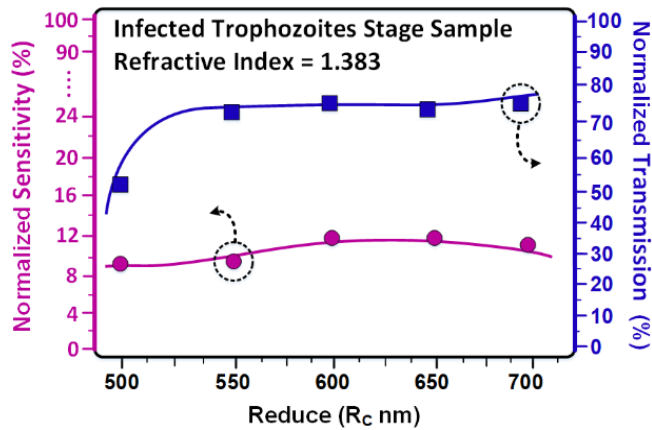


Fig. 7. Sensitivity and Transmission in terms of different radius of the glass cylinder.

From Figures 6 and 7, it can be concluded that the best radius for the glass cylinder is 600nm, with the highest transmission of 97% and the best sensitivity in Infected Ring Stage sample equal to 11.91RIU<sup>-1</sup>. Another important advantage of the small size of the proposed structure is that it significantly increases the speed in the detected performance.

## 5. Conclusion

In this work, an all-optical biosensor based on the refractive index is designed and simulated for the detection of malaria disease in two-dimensional photonic crystals (2D-PhCs). The reason for choosing to detect malaria is its dangerousness and attention lack in the design of all-optical biosensors in photonic crystals. The proposed biosensor operates according to the intensity of the optical signal field in the output waveguide. Due to the refractive index of the samples, the intensity of the optical signal field changes. Most of the transmissions are related to a sample of a healthy person with 97% and the lowest amount is related to an Infected Schizont Stage sample of 66.12%. Optical signal power loss is 3% at best and 33.88% at worst. The sensitivity parameter for the best case (infected trophozoite stage sample) is equal to 11.91RIU<sup>-1</sup> and for the worst case (Infected Ring Stage sample) is equal to 8.21RIU<sup>-1</sup>. Due to the small size of the structure, it can be integrated, which is equal to 57 $\mu$ m<sup>2</sup>. For future study, some recommendations can be explored as, conducting experimental validation to verify the simulation results and assess the biosensor's real-world performance. This would involve performing tests on a larger set of clinical samples from individuals with different stages of malaria to evaluate the biosensor's accuracy and diagnostic capabilities. Moreover, exploring strategies to enhance the sensitivity of the biosensor for improved detection. This could include investigating novel materials, optimizing design

parameters, or incorporating additional functional elements to increase the biosensor's sensitivity. Additionally, miniaturization and integration efforts should be pursued to develop a compact and portable biosensor suitable for point-of-care testing in resource-limited settings. By addressing these recommendations, future studies can advance the field of malaria detection and contribute to the development of more efficient and reliable biosensors for disease diagnostics.

## REFERENCES

- [1] W. Bogaerts, and L. Chrostowski, "Silicon photonics circuit design: methods, tools and challenges," *Laser & Photonics Reviews*, vol. 12, no. 4. 1700237, April 2018.
- [2] M. Hosseinzadeh Sani, and S. and Khosroabadi. "A novel design and analysis of high-sensitivity biosensor based on nano-cavity for detection of blood component, diabetes, cancer and glucose concentration," *IEEE Sensors Journal*. 20.13. pp. 7161-7168. April 2020.
- [3] M. Hosseinzadeh Sani, A. Ghanbari, and H. Saghaei. "High-sensitivity biosensor for simultaneous detection of cancer and diabetes using photonic crystal microstructure," *54(1):1-4*. pp.1-14. Janary 2021.
- [4] Q. Gong, and X. Hu, *Photonic crystals: principles and applications*, 1st ed. Jenny Stanford Publishing, 6, February 2013.
- [5] S. M. Musavizadeh, M. Soroosh, and F. Mehdizadeh, "Optical filter based on photonic crystal," *Indian Journal of Pure & Applied Physics*, vol. 53, no. 11, pp. 736–739, April 2015.
- [6] M. Hosseinzadeh Sani, A Ghanbari, and H Saghaei. "An ultra-narrowband all-optical filter based on the resonant cavities in rod-based photonic crystal microstructure," *Optical and Quantum Electronics* 52: 1-15. June 2020.
- [7] D. Qi, X. Wang, Y. Cheng, F. Chen, L. Liu, and R. Gong, "Quasi-periodic photonic crystal Fabry–Perot optical filter based on Si/SiO<sub>2</sub> for visible-laser spectral selectivity," *Journal of Physics D: Applied Physics*, vol. 51, no. 22, 225103, May 2018.

- [8]R. Talebzadeh, M. Soroosh, Y. S. Kavian, and F. Mehdizadeh, "Eight-channel all-optical demultiplexer based on photonic crystal resonant cavities," *Optik*, vol. 140, pp. 331-337, July 2017.
- [9]V. Fallahi, M. Seifouri, S. Olyaei, and H. Alipour-Banaei, "Four-channel optical demultiplexer based on hexagonal photonic crystal ring resonators," *Optical Review*, vol. 24, no. 4, pp. 605-610, August 2017.
- [10]M. Hosseinzadeh Sani, A. A. Tabrizi, H. Saghaei, and R. Karimzadeh, "An ultrafast all-optical half adder using nonlinear ring resonators in photonic crystal microstructure," *Optical and Quantum Electronics* 52.2: 1-10. February 2020.
- [11]P. Sami, C. Shen, and M. Hosseinzadeh Sani. "Ultra-fast all optical half-adder realized by combining AND/XOR logical gates using a nonlinear nanoring resonator," *Applied Optics* 59.22: 6459-6465. August 2020.
- [12]S. Serajmohammadi, H. Alipour-Banaei, and F. Mehdizadeh, "Proposal for realizing an all-optical half adder based on photonic crystals," *Applied Optics*, vol. 57, no. 7, pp. 1617-1621, March 2018.
- [13]S. S. Zamanian-Dehkordi, M. Soroosh, and G. Akbarizadeh, "An ultra-fast all-optical RS flip-flop based on nonlinear photonic crystal structures," *Optical Review*, vol. 25, no. 4, pp. 523-531, August 2018.
- [14]T. A. Moniem, "All-optical S-R flip flop using 2-D photonic crystal," *Optical and Quantum Electronics*, vol. 47, no. 8, pp. 2843-2851, August 2015.
- [15]M. Hosseinzadeh Sani, S. Khosroabadi, and A. Shokouhmand. "A novel design for 2-bit optical analog to digital (A/D) converter based on nonlinear ring resonators in the photonic crystal structure," *Optics Communications* 458: 124760. March 2020.
- [16]M. Hosseinzadeh Sani, S. Khosroabadi, and M. Nasserian. "High performance of an all-optical two-bit analog-to-digital converter based on Kerr effect nonlinear nanocavities," *Applied optics* 59.4: 1049-1057. February 2020.
- [17]Jiu-Sheng L, Han L, Le Z. "Compact four-channel terahertz demultiplexer based on directional coupling photonic crystal," *Opt Commun*; 350:248-51. September 2015.
- [18]Pitruzzello G, Krauss TF. "Photonic crystal resonances for sensing and imaging," *J Opt*; 20:073004. June 2018.
- [19]Zaky ZA, Aly AH. "Theoretical study of a tunable low-temperature photonic crystal sensor using dielectric-superconductor nanocomposite layers. *J Supercond Nov Magn*. 2020; 33:2983-90, October 2020.
- [20]Abd El-Ghany SE, Noum WM, Matar Z, Zaky ZA, Aly AH. "Optimized bio-photonic sensor using 1D-photonic crystals as a blood hemoglobin sensor," *Phys Scr*. ;96:035501. February 2020.
- [21]Zaky ZA, Aly AH. "Modeling of a biosensor using Tamm resonance excited by graphene," *Appl Opt*; 60:1411-9, February 2021.
- [22]Barillaro G, Merlo S, Surdo S, Strambini LM, Carpignano F. "Integrated optofluidic microsystem based on vertical highorder one-dimensional silicon photonic crystals. *Microfluid Nanofluidics*," 12:545-52. January 2012.
- [23]K. Haldar, S. Kamoun, N. L. Hiller, S. "Bhattacharje and C. van Ooij, *Nat. Rev. Microbiol*, 4, 922-931. December 2006.
- [24]I. Weissbuch and L. Leiserowitz, *Chem. Rev*, 108, 4899-4914. November 2008.